Physiol. Meas.

Smartphone-based remote assessment of upper extremity function for multiple sclerosis using the Draw a Shape Test

A. P. Creagh[1,2], C. Simillion[2], A. Scotland[2], F. Lipsmeier[2], C. Bernasconi[2], S. Belachew[2], J. van Beek[2], M. Baker[2], C. Gossens[2], M. Lindemann[2‡] and M. De Vos[1‡]

[1] Institute of Biomedical Engineering, University of Oxford, UK;
[2] F. Hoffmann-La Roche Ltd., Basel, CH;
[‡] Shared last authorship.

E-mail: andrew.creagh@eng.ox.ac.uk

1. Supplementary Material

1.1. Distribution of the Nine-Hole Peg Test (9HPT)

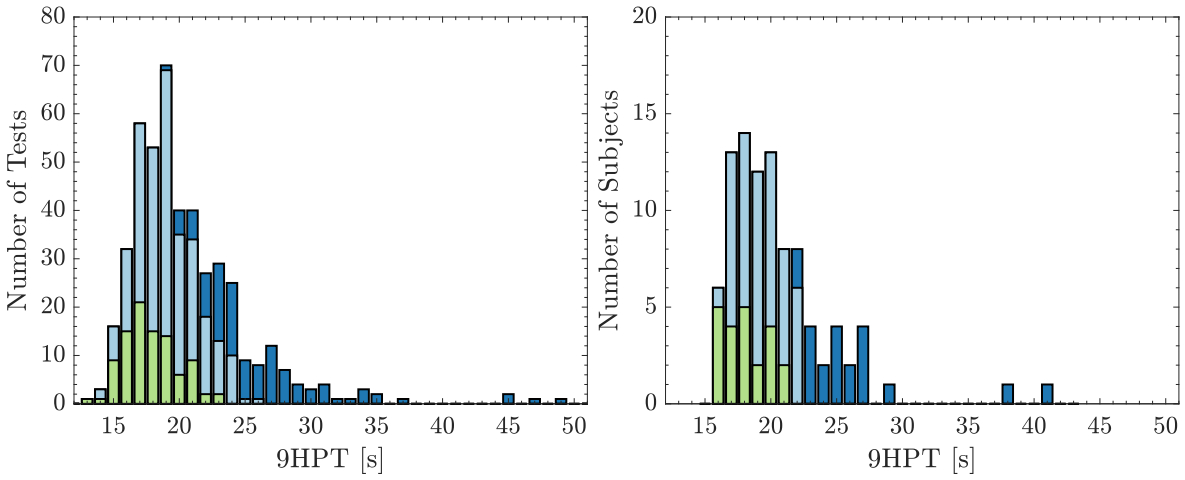

(a) All 9HPTs (b) Average 9HPT

Figure 1: Distribution of (a) all Nine-Hole Peg Test (9HPT) times [s] from all 3 clinical visits for pooled dominant and non-dominant handed tests, and coloured by subject group and (b) average Nine-Hole Peg Test time (9HPT) [s] per subject from all 3 clinical visits for pooled dominant and non-dominant handed tests, and coloured by subject group. HC are shown in green. PwMS were grouped into presumably normal (nPwMS) versus abnormal (aPwMS) hand/arm function based on an upper limit of normal range, defined as the averge 9HPT times for HCs plus two standard deviations over pooled dominant and non-dominant handed tests. nPwMS are shown in light blue, and aPwMS are depicted in dark blue.

1.2. Description of features relating to upper-extremity function extracted from the Draw-a-Shape Test

Raw sensor data is collected from the smartphone touchscreen during the active Draw a Shape Test and stored as x- and y-screen coordinates with a corresponding timestamp t: (x, y, t), where N is the total number of touch data points. Features were extracted from various shapes such as the (*circle*, *figure-8-shape*, *spiral*, *square*) traced on smartphone touchscreen. Drawing velocity (v) is calculated using [1]:

$$v = \sum_{i=1}^{N-1} \frac{\sqrt{(x_{i+1} - x_i)^2 - (y_{i+1} - y_i)^2}}{t_{i+1} - t_i}$$

Radial velocity (RV) is also calculated, using the following equation [1]:

$$RV = \sum_{i=1}^{N-1} \frac{r_{i+1} - r_i}{t_{i+1} - t_i}$$

where r is the radius, defined by: $\sqrt{(x^2 + y^2)}$.
Angular velocity (RHOV) is also calculated, using the following equation [1]:

$$RV = \sum_{i=1}^{N-1} \frac{\theta_{i+1} - \theta_i}{t_{i+1} - t_i}$$

where $\theta = \text{atan}_2(\frac{y}{x})$ and atan_2 is the four-quadrant inverse tangent, $\tan^{-1}(\frac{y}{x})$.
All features calculated on v were also computed using the RV and $RHOV$.
Touch screen x- and y- coordinates can be converted to a grayscale achromatic intensity image IM that contain values in the range 0 (black) to 1 (white). Coordinates are first scaled to the original resolution of the smartphone used. IM_{ref} refers to the reference shape x- and y-coordinates interpolated to fixed length L and converted to a grayscale intensity image.
Discretized heat maps of touch events, HM, described in the methods section of the accompanying paper are referred to with the prefix *"Spatiotemporal"* before the feature name. Those heat maps constructed with reference coordinates are referred to as HM_{ref}. *All features calculated on IM are also computed using the HM images.

The table below describes all features extracted from the Draw-a-Shape Test.
Features which were extracted on all shapes are denoted using, ⟨ *shape* ⟩ reference. Those features that are shape dependent reference the specific shape that the feature was extracted on. ⟨ *overall* ⟩ refers to any feature computed over all shapes, where the value was taken as the mean or sum over all shapes, which are detailed and referenced accordingly in table 1.

Table 1: Description of features relating to upper-extremity function extracted from the Draw-a-Shape Test

Shape	Feature	Description
⟨ *shape* ⟩	acc	The total number of successfully passed waypoints divided by the number of waypoints per shape.
⟨ *shape* ⟩	$apen(v)$	The approximate entropy of v. Time-series x is first interpolated to a fixed length L and using the parameters defined in [1, 2].
⟨ *shape* ⟩	$asym(x, y)$	Shape asymmetry in the x- and y- plane [1].
⟨ *shape* ⟩	$AUC(x, y)$	Drawing error as represented by area-under-the-curve (AUC) integration using the trapezoidal method with unit spacing over the drawn-touch points with respect to the touch coordinates. Using similar methodology to [3].
⟨ *shape* ⟩	$iqr(AUC(x, y))$	The interquartile range of the AUC.
⟨ *circle*, *spiral* ⟩	$AUC_{CS}(x, y)$	The mean AUC error in the circular shapes.
⟨ *line*, *square* ⟩	$AUC_{LS}(x, y)$	The mean AUC error in the line & square shapes.
⟨ *shape* ⟩	$celerity(x, y, t)$	Celerity, defined as the ratio of successfully passed waypoints divided by the time taken to complete the shape.
⟨ *circle*, *spiral* ⟩	$celerity_{CS}(x, y, t)$	The mean celerity in the circular shapes.
⟨ line, *square* ⟩	$celerity_{LS}(x, y, t)$	The mean celerity in the line and square shapes.
⟨ *figure-8-shape* ⟩	$centre_{offshoot}(x, y)$	Euclidean distance by which the touch coordinates misses the centre of the shape.
⟨ *overall* ⟩	$completedRate1$	The number of shapes successfully completed on the first attempt, divided by the total number of attempts.
⟨ *overall* ⟩	$completedRate2$	The number of shapes successfully completed on the second attempt, divided by the total number of attempts.
⟨ *overall* ⟩	$completedRate$	The number of shapes successfully completed on the first attempt and on the second attempt, divided by the total number of attempts.
⟨ *shape* ⟩	$corr(IM, IM_{ref})$	The 2-D image correlation coefficient between shape drawn and reference shape image [4].
⟨ *shape* ⟩	$cov(v)$	The coefficient of variation in v.
⟨ *shape* ⟩	$var(v)$	The variance in v.

$\langle$ *shape* $\rangle$	$drawPathRMSE(x, y)$	The root-mean-squared errror (RMSE) between the square root of the x- and y- touch points squared and the square root of the x- and y- reference points squared, similar to [1].
$\langle$ *shape* $\rangle$	*dwell-to-move*(x, y)	The ratio of total dwell time to total time taken to complete the SQUARE shape. See dwellTime feature.
$\langle$ *square* $\rangle$	$dwellTime(x, y)$	Dwell time is used as a measure to assess hesitation time ability to change direction at the corners of square shapes. Velocity (v) is first calculated as described previously, where the local maxima in v represent local max drawing speed and local minima represent the stoppages. Dwell time is calculated as the time distance (width) at half the corresponding minima height.
$\langle$ *square* $\rangle$	$dwellTime_m(x, y)$	Mean dwell time. See dwellTime feature.
$\langle$ *square* $\rangle$	$dwellTime_{sd}(x, y))$	The standard deviation in the dwell time. See $dwellTime$ feature.
$\langle$ *spiral* $\rangle$	$GOF(x, y)$	RMSE value calculated linear regression between ideal (reference) and drawn touch coordinates. See [5] for more details.
$\langle$ *shape* $\rangle$	$HausD(x, y)$	The maximum Hausdorff distance between drawn and reference shape which is assessed as an approximate for maximum drawing error[6, 7].
$\langle$ *shape* $\rangle$	$HausDError(x, y)$	The sum of the Hausdorff distances (largest minimum distance to closest iterative points) between drawn and reference shape, normalised by the number of touchpoints.
$\langle$ *shape* $\rangle$	$HausD_{25}(x, y)$	The sum of the Hausdorff distances (largest minimum distance to closest iterative points) between drawn and reference shape, normalised by the number of touchpoints - assessed as an approximate for drawing error at start of drawing.
$\langle$ *shape* $\rangle$	$HausD_{75}(x, y)$	The sum of the Hausdorff distances (largest minimum distance to closest iterative points) between drawn and reference shape, normalised by the number of touchpoints - assessed as an approximate for drawing error at end of drawing.

$\langle$ *shape* $\rangle$	$hausD_t(x, y)$	The Hausdorff distance normalised by the time taken to draw the shape.
$\langle$ *shape* $\rangle$	$hausDmiddle(x, y)$	Hausdorff distance using touch coordinates from the middle of drawing (i.e. 15-85% range).
$\langle$ *shape* $\rangle$	$hausDmiddle_t(x, y)$	Hausdorff distance using touch coordinates from the middle of drawing (i.e. 15-85% range) weighted by the time taken to complete the shape.
$\langle$ *shape* $\rangle$	$HD_E(IM, x, y)$	Image entropy of IM multiplied (*) by the maximum Hausdorff Distance as a measures of penalised drawing irregularity.
$\langle$ *shape* $\rangle$	$cov(hf(v))$	The variance of the high-frequency wavelet coefficients of v. The high frequency components are first extracted by a 1-level Discrete Wavelet Transform (DWT) using Daubechies 10 wavelet function. This is proposed as a feature for detecting the variation in short and fast movement changes during the spiral drawing task [1].
$\langle$ *shape* $\rangle$	$hf_m(v)$	The mean high-frequency wavelet coefficients of x. The high frequency components are first extracted by a 1-level Discrete Wavelet Transform (DWT) using Daubechies 10 wavelet function, similar to [1].
$\langle$ *shape* $\rangle$	$max(hf(v))$	The maximum high-frequency wavelet coefficients of v. The high frequency components are first extracted by a 1-level Discrete Wavelet Transform (DWT) using Daubechies 10 wavelet function.
$\langle$ *shape* $\rangle$	$hf_{sd}(v)$	The standard deviation in the high-frequency wavelet coefficients of v. The high frequency components are first extracted by a 1-level Discrete Wavelet Transform (DWT) using Daubechies 10 wavelet function, similar to [1].
$\langle$ *shape* $\rangle$	$ImEntropy(IM)$	Image entropy of shape drawn [8].
$\langle$ *shape* $\rangle$	$\frac{ImEntropy(IM)}{ImEntropy(IM_{ref})}$	Image entropy of shape drawn with respect to reference shape [8].
$\langle$ *shape* $\rangle$	$imRatio(IM, IM_{ref})$	Mean pixel intensity ratio between shape drawing transposed as pixel density heat map and reference image.

⟨ *shape* ⟩	$iqr(HausD)$	Interquartile range of Hausdorff distance computed between drawn touch points and reference coordinates. See hausD.
⟨ *shape* ⟩	$isdRatio(IM, IM_{ref})$	Standard deviation in the pixel intensity ratio between shape drawing and reference shape.
⟨ *shape* ⟩	$kurt(v)$	Kurtosis as a measure of the taildness of the probability distribution of v values, and is used as a measure of how outlier prone a distribution is.
⟨ *shape* ⟩	$max(v)$	The maximum velocity, v.
⟨ *shape* ⟩	$\max(t_{pixel}(x, y))$	Maximum hesitation time [s], defined as the maximum time a finger remains in one (x, y) coordinate regions, which are defined by the binning of touch events into discretized heat maps.
⟨ *shape* ⟩	$mean(v)$	The mean of v [9, 10]
⟨ *overall* ⟩	$celerity_m$	The mean celerity over all shapes, defined as the ratio between the number of successfully completed way-points and the time taken to complete the shape.
⟨ *shape* ⟩	$MI(IM, IMref)$	The mutual information between the shape drawing touch coordinates and reference coordinate [11, 12].
⟨ *shape* ⟩	$mIm(IM)$	Mean pixel intensity for shape drawing image.
⟨ *shape* ⟩	$mPeak(v)$	The mean number of peaks in v [1].
⟨ *shape* ⟩	$mPI(IM)$	Mean pixel intensity for shape drawing image.
⟨ *shape* ⟩	$nMSE$	The 2-D mean square error between shape drawing touch coordinates and reference coordinate [13].
⟨ *shape* ⟩	$nPeaks(v)$	The number of peaks in v [1].
⟨ *shape* ⟩	$nPeaksNorm(v)$	The number of peaks in v, normalised by the number of samples in v. This has been proposed as a measure of fine drawing control [1].
⟨ *shape* ⟩	$nRMSE$	The 2-D root-mean square error between shape drawing touch coordinates and reference coordinate [13].
⟨ *shape* ⟩	$numHits$	Number of successfully passed waypoints.
⟨ *circle*, *spiral* ⟩	$numHits_{CS}$	The total number of waypoint hits in the circular shapes.
⟨ *line*, *square* ⟩	$numHits_{LS}$	The total number of hits in the line & square shapes.

⟨ *square* ⟩	$overShoot(x, y)$	The total Euclidian distance error by which a subject overshoots or undershoots (misses) a corner.
⟨ *shape* ⟩	$overShoot_m(x, y)$	The mean Euclidian distance error by which a subject overshoots or undershoots (misses) over all 4 corners.
⟨ *shape* ⟩	$overShoot_{sd}(x, y)$	The variance in the Euclidian distance error by which a subject overshoots or undershoots (misses) a corner over all over all 4 corners, as measured by the standard deviation.
⟨ *shape* ⟩	$pDchisq(v)$	The Chi-square distance between the two histograms of heatmap transposed pixel intensity counts which can be used as a rough similarity index [14, 15].
⟨ *shape* ⟩	$pSNR(IM)$	The peak signal-to-noise ratio between in shape drawn with the ideal (reference) touch coordinates [13].
⟨ *shape* ⟩	$\max(PSD(v))$	Maximum Power Spectral Density (PSD) estimate of v, computed using a Welsh periodogram with a Hamming window. Similar to [16].
⟨ *shape* ⟩	$\arg\max_f(PSD(v))$	The dominant frequency refers to the frequency which maximises the Power Spectral Density (PSD) estimate of v.
⟨ *shape* ⟩	$pRMS(v)$	Root-mean squared value of v.
⟨ *spiral* ⟩	$R_{lfit}(x, y)$	r^2 (adjusted) value calculated linear regression between ideal (reference) and drawn touch coordinates. See [5] for more details.
⟨ *overall* ⟩	shp_c	The number of the correctly completed shapes over a test instance, regardless of attempt number.
⟨ *overall* ⟩	shp_{fail}	The number of failed shape drawing attempts over a test instance.
⟨ *shape* ⟩	$skew(v)$	The skewness of distribution of v.
⟨ *shape* ⟩	$sp(v)$	Spearman's rank correlation (R_{sp}) coefficient of the level of variation with time of v. This is computed as the change of variation over time in number of peaks during a test trial, calculated using a sliding window, which compared standard deviations over 30 overlapping windows. For more details we refer the reader to the original description in [1]

$\langle$ *shape* $\rangle$	$SSI(IM, IM_{ref})$	Structural Similarity Index, as described in [17].
$\langle$ *shape* $\rangle$	$std(v)$	The standard deviation of v [10].
$\langle$ *shape* $\rangle$	$time$	Total time taken to complete the shape.
$\langle$ *shape* $\rangle$	$TOTSYMM(x, y)$	Total summation of the shape asymmetry in the x-plane and y-plane [1].

1.3. Inter-shape and intra-shape feature correlation

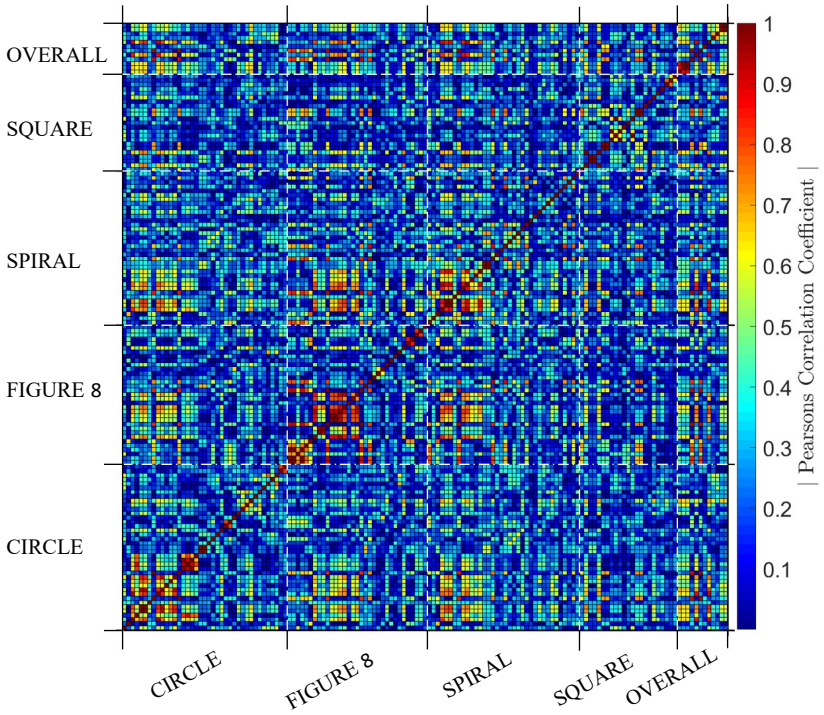

Figure 2: Pairwise linear Pearson's (R_{ps}) correlation matrix, showing the intra-shape, and inter-shape absolute feature correlation for the top shape features (n=144). Top features were deduced as those features with univariate correlation to the 9HPT [s], $R_{ps} > 0.25$, $P < 0.05$. Feature values are taken as the median feature value per subject (n=93) where the corresponding 9HPT was computed as the average 9HPT per subject over the entire study. It was exhibited that collinearity existed within the shape features, and across shape features, highlighting the need for proficient regularisation. Of the top ranked shape features, *circle* features contribute (n=39), *figure-8-shape* (n=33), *spiral* (n=36), *square*(n=23) and *overall* performance metrics (n=13). Please note, FIGURE 8 refers to the *figure-8-shape* drawn by subjects.

References

[1] Mevludin Memedi, Aleksander Sadikov, Vida Groznik, Jure Žabkar, Martin Možina, Filip Bergquist, Anders Johansson, Dietrich Haubenberger, and Dag Nyholm. Automatic spiral analysis for objective assessment of motor symptoms in parkinson's disease. *Sensors (Basel, Switzerland)*, 15(9):23727–23744, 2015.

[2] M. Memedi, S. Aghanavesi, and J. Westin. A method for measuring parkinson's disease related temporal irregularity in spiral drawings. In *2016 IEEE-EMBS International Conference on Biomedical and Health Informatics (BHI)*, pages 410–413.

[3] Somayeh Aghanavesi, Dag Nyholm, Marina Senek, Filip Bergquist, and Mevludin Memedi. A smartphone-based system to quantify dexterity in parkinson's disease patients. *Informatics in Medicine Unlocked*, 9:11–17, 2017.

[4] Robert M Haralick and Linda G Shapiro. *Computer and robot vision*, volume 1.

[5] Mitchell Grant Longstaff and Richard A Heath. Spiral drawing performance as an indicator of fine motor function in people with multiple sclerosis. *Human movement science*, 25(4):474–491, 2006.

[6] M-P Dubuisson and Anil K Jain. A modified hausdorff distance for object matching. In *Pattern Recognition, 1994. Vol. 1-Conference A: Computer Vision Image Processing., Proceedings of the 12th IAPR International Conference on*, volume 1, pages 566–568. IEEE.

[7] Daniel P. Huttenlocher, Gregory A. Klanderman, and William J Rucklidge. Comparing images using the hausdorff distance. *IEEE Transactions on pattern analysis and machine intelligence*, 15(9):850–863, 1993.

[8] Du-Yih Tsai, Yongbum Lee, and Eri Matsuyama. Information entropy measure for evaluation of image quality. *Journal of Digital Imaging*, 21(3):338–347, 2008.

[9] Xuguang Liu, Camille B. Carroll, Shou-Yan Wang, John Zajicek, and Peter G. Bain. Quantifying drug-induced dyskinesias in the arms using digitised spiral-drawing tasks. *Journal of Neuroscience Methods*, 144(1):47–52, 2005.

[10] S. Wang, P. G. Bain, T. Z. Aziz, and X. Liu. The direction of oscillation in spiral drawings can be used to differentiate distal and proximal arm tremor. *Neurosci Lett*, 384(1-2):188–92, 2005.

[11] Josien PW Pluim, JB Antoine Maintz, and Max A Viergever. Mutual-information-based registration of medical images: a survey. *IEEE transactions on medical imaging*, 22(8):986–1004, 2003.

[12] Frederik Maes, Andre Collignon, Dirk Vandermeulen, Guy Marchal, and Paul Suetens. Multimodality image registration by maximization of mutual information. *IEEE transactions on Medical Imaging*, 16(2):187–198, 1997.

[13] J-C Yoo and CW Ahn. Image matching using peak signal-to-noise ratio-based occlusion detection. *IET image processing*, 6(5):483–495, 2012.

[14] Manesh Kokare, BN Chatterji, and PK Biswas. Comparison of similarity metrics for texture image retrieval. In *TENCON 2003. Conference on convergent technologies for Asia-Pacific region*, volume 2, pages 571–575. IEEE.

[15] Wei Yang, Luhui Xu, Xiaopan Chen, Fengbin Zheng, and Yang Liu. Chi-squared distance metric learning for histogram data. *Mathematical Problems in Engineering*, 2015, 2015.

[16] Lutz-Peter Erasmus, Stefania Sarno, Holger Albrecht, Martina Schwecht, Walter Pöllmann, and Nicolaus König. Measurement of ataxic symptoms with a graphic tablet: standard values in controls and validity in multiple sclerosis patients. *Journal of Neuroscience Methods*, 108(1):25–37, 2001.

[17] Zhou Wang, Alan C Bovik, Hamid R Sheikh, and Eero P Simoncelli. Image quality assessment: from error visibility to structural similarity. *IEEE transactions on image processing*, 13(4):600–612, 2004.